Evgeny V. Nazarchuk, Oleg I. Siidra*, Yana G. Tagirova, Dmitri O. Charkin, Dmitri N. Dmitriev and Anatoly V. Kasatkin

Thermal evolution of soddyite, $(UO_2)_2SiO_4(H_2O)_2$ and structurally related $Na_2(UO_2)_2SiO_4F_2$

https://doi.org/10.1515/zkri-2024-0091
Received June 15, 2024; accepted November 29, 2024;
published online January 27, 2025

Abstract: Thermal expansion of the mineral soddyite, $(UO_2)_2SiO_4(H_2O)_2$, and structurally related synthetic compound $Na_2(UO_2)_2SiO_4F_2$ (***NAUSIF***) has been studied by means of high-temperature single-crystal and powder X-ray diffraction. The mineral is orthorhombic, *Fddd*, while ***NAUSIF*** is tetragonal, $I4_1/amd$. The framework structures of both compounds are comprised of either neutral $[(UO_2)_2(SiO_4)(H_2O)_2]$ or negatively charged $[(UO_2)_2(SiO_4)F_2]^{2-}$ chains of similar topology. In the structure of soddyite, the chains cross at the angle of 72°, while in ***NAUSIF*** of 90°. Upon increasing temperature, the acute inter-chain angles in soddyite increase due to hinge deformations, the overall symmetry approaching tetragonal. The mineral is stable below 325 ± 25 °C; between 325 and 640 °C, the decomposition products cannot be identified unambiguously and contain significant amount of amorphous phases; at higher temperatures, a mixture of U_3O_8 polymorphs is formed. ***NAUSIF*** is stable until its melting point of 625 ± 25 °C. The thermal expansion of both compounds is strongly anisotropic; for ***NAUSIF***, it is due to difference in bond strength in the uranium and sodium polyhedra. Anisotropic thermal expansion of soddyite is controlled by shear deformations of the structure upon the temperature rise.

Keywords: uranium; silicates; fluorides; soddyite; thermal evolution; thermal expansion

1 Introduction

Investigations of the oxidation products of uraninite UO_2[1–3] are of essential importance for proper understanding the evolution of both mineral formation upon oxidation of uranium deposits and alteration of spent nuclear fuel.[4] Temperature is one of the key parameters affecting the stability of uranium compounds. Thermodynamic modeling of uraninite dissolution in silica-saturated groundwaters indicate that the process is controlled by formation of several uranyl compounds including soddyite $(UO_2)_2SiO_4(H_2O)_2$.[5] Studies of mineral associations of uranium deposits oxidation areas demonstrate that interaction of fluids with rocks upon weathering produces several uranyl silicates including uranophane $Ca[(UO_2)(SiO_3OH)]_2(H_2O)_5$, boltwoodite $(K,Na)[(UO_2)(SiO_3OH)](H_2O)_{1.5}$, haiweeite $Ca[(UO_2)_2Si_5O_{12}(OH)_2](H_2O)_3$, and soddyite.[1,6–8]

Soddyite was first described by Schoep in 1922; its first X-ray study was performed by Gorman in 1952. The mineral was found to be orthorhombic, a = 8.32 Å, b = 11.21 Å, c = 18.71 Å, space group *Fddd*.[9] Legros et al.[10] prepared $2UO_3{\cdot}GeO_2{\cdot}2H_2O$ and $2UO_3{\cdot}SiO_2{\cdot}2H_2O$ and demonstrated the silicate and the germanate to be isostructural; the structure of the latter was determined in 1975.[10] Later on, the crystals of synthetic soddyite were prepared by Kuznetsov et al.[11], Moll [12] and Belokoneva et al.[13] In the latter work, the structure of the synthetic compound was solved to R_1 = 0.021 and wR_1 = 0.029 but hydrogen atoms were not localized. Attempts were also made to solve the structure from PND data.[14] Demartin et al.[15] Localized hydrogen positions and refined the structure down to $R1$ = 6.4 %. The latest study by Plášil et al.[16] confirmed the *Fddd* space group and the unit cell parameters were a = 8.3097(3) Å, b = 11.2205(4) Å, c = 18.6575(11) Å, R_1 = 1.9 %.

Both synthetic and natural soddyite crystals were analyzed by a variety of techniques. Čejka[17] analyzed the IR spectroscopy data, while Frost[18] and Colmenero[19] provided the Raman spectra and DFT calculations. Particular attention was paid to the thermal properties of the mineral. The first decomposition stage of soddyite and its germanate analog at *ca.* 460 °C was found to correspond to the total dehydration and formation of amorphous products.[20] Formation of the latter was explained by the arising

Dedicated to Professor Dr. Dr. h. c. Wulf Depmeier on the occasion of his 80th birthday.

***Corresponding author: Oleg I. Siidra**, Department of Crystallography, Saint-Petersburg State University, University emb. 7/9, St., Petersburg 199034, Russia; and Institute of Silicate Chemistry, Russian Academy of Sciences, Makarova Emb. 2, St Petersburg 199034, Russia, E-mail: o.siidra@spbu.ru
Evgeny V. Nazarchuk and Yana G. Tagirova, Department of Crystallography, Saint-Petersburg State University, University Emb. 7/9, St., Petersburg 199034, Russia
Dmitri O. Charkin and Dmitri N. Dmitriev, Department of Chemistry, Moscow State University, Vorobievy Gory 1, Bd. 3, Moscow 119991, Russia
Anatoly V. Kasatkin, Fersman Mineralogical Museum of the Russian Academy of Sciences, Leninskiy Pr. 18, 2, 119071, Moscow, Russia

under-saturation of the uranyl cation due to the removal of coordinated water from the $(UO_2)O_4(H_2O)$ pentagonal bipyramid.[21] The second stage of soddyite decomposition at *ca*. 640 °C corresponds to the release of oxygen and uranium reduction to the tetravalent state with crystallization of coffinite analog, $USiO_4$. Though the thermal behavior of soddyite is well studied, no reference data could be found concerning its thermal expansion. The data on polythermic studies of the synthetic soddyite were provided by Sureda et al.[22] and interpreted only as an illustration to the staged dehydration process. Synthetic soddyite was reported to lose water at 400 °C with subsequent melting at 470° C.

Blaton et al.[23] reported hydrothermal synthesis of $Na_2(UO_2)_2SiO_4F_2$. Its crystal structure is derived from soddyite by replacing water molecules by the fluoride anions and filling the channels by the sodium cations; otherwise, the topologies of these frameworks are identical.

In the current study, the thermal behavior and particularly expansion of soddyite and $Na_2(UO_2)_2SiO_4F_2$ (***NAUSIF*** further on) were probed by a set of variable-temperature single-crystal and powder diffraction methods.

2 Experimental

2.1 Samples and occurrence

Soddyite originates from Swambo Hill, Haut-Katanga, DR Congo. It occurs as canary-yellow blocky and platy crystals up to 0.3 mm across (Figure 1a and b) and associates with curite, goethite and kaolinite.

2.2 Synthesis

Caution! Although the uranium precursors used contain depleted uranium, standard safety measures for handling radioactive substances must be followed.

As we had reported earlier,[24] single crystals of uranyl silicates can be readily prepared from uranium oxides and silica via “activation” by reactive fluorides. The crystals of ***NAUSIF*** (Figure 1c and d) were produced from a mixture of 22 mg of NaF (Vecton, 99.7 %) and 52 mg U_3O_8 (Vecton, 99.7 %) pre-dried at 80 °C. The reagents were additionally activated. This mixture was transferred to a silica tube (which served also as the source of silicon), then 30 µL of 40 % hydrofluoric acid was injected. After 1 min, the tube was attached to a vacuum line, evacuated, and sealed. The silica tube was heated to 950 °C at a rate of 70 °C/h, soaked for 99 h, and cooled to room temperature at the rate of 5 °C/h.

2.3 Single-crystal X-ray studies

Single-crystal X-ray data of soddyite and ***NAUSIF*** were collected using a Rigaku XtaLAB Synergy-S diffractometer equipped with a PhotonJet-S detector operating with MoKα radiation at 50 kV and 1 mA. A single crystal was chosen and more than a hemisphere of data collected with a frame width of 0.5° in ω, and 25 s spent counting for each frame. The data were integrated and corrected for absorption applying a multi-scan type model using the Rigaku Oxford Diffraction programs CrysAlis Pro 1.1.11.

The ***NAUSIF*** crystal was studied in the temperature range of 25–725 °C using a «Hot Air Gas Blowers » heating system. The structures were successfully refined with the use of SHELX software package.[25] Atom coordinates and thermal displacement parameters for each temperature are collected in the corresponding cif files (Supplement 1); experimental parameters are provided in Table 1. Unit-cell parameters are given for 25 °C. The procedure of variable-temperature single-crystal X-ray study is in that the crystal is placed in a silica capillary and thermostated before each data collection. Therefore, temporal restrictions and essential lowering of reflection intensities due to extinction by capillary walls require the use of relatively large crystals. Unfortunately, due to hydration and intergrowths twinning, just two acceptable soddyite crystals could be picked out of the natural samples; ever those were so small that full data collection would require more than 14 h. Hence, PXRD studies were the only possible way for investigating the thermal evolution of soddyite. In the meantime, the ***NAUSIF*** crystals provided by high-temperature technique were quite large and well-grained crystals excellent for the capillary experiments.

The effect of thermal motion on the bond-length values from single-crystal X-ray diffraction experiments is well-known.[26] Corrections for all bonds in the studied compounds were calculated by using a formula for the rigid-body motion:

$$L^2 = l_0^2 + \frac{3}{8}\pi^2 \left(B_{eq}(A_2) - B_{eq}(A_1)\right)$$

Where L and l_0 are corrected and observed A_1–A_2 bond lengths, respectively; $B_{eq}(A_1)$ and $B_{eq}(A_2)$ are equivalent temperature factors of A_1 (cation, i.e. U, Si, Na) and A_2 (anion i.e. O, F) atoms, respectively.

2.4 Chemical composition

The chemical analysis of soddyite was carried out with a Hitachi FlexSEM 1,000 scanning electron microscope equipped with EDS Xplore Contact 30 detector and Oxford

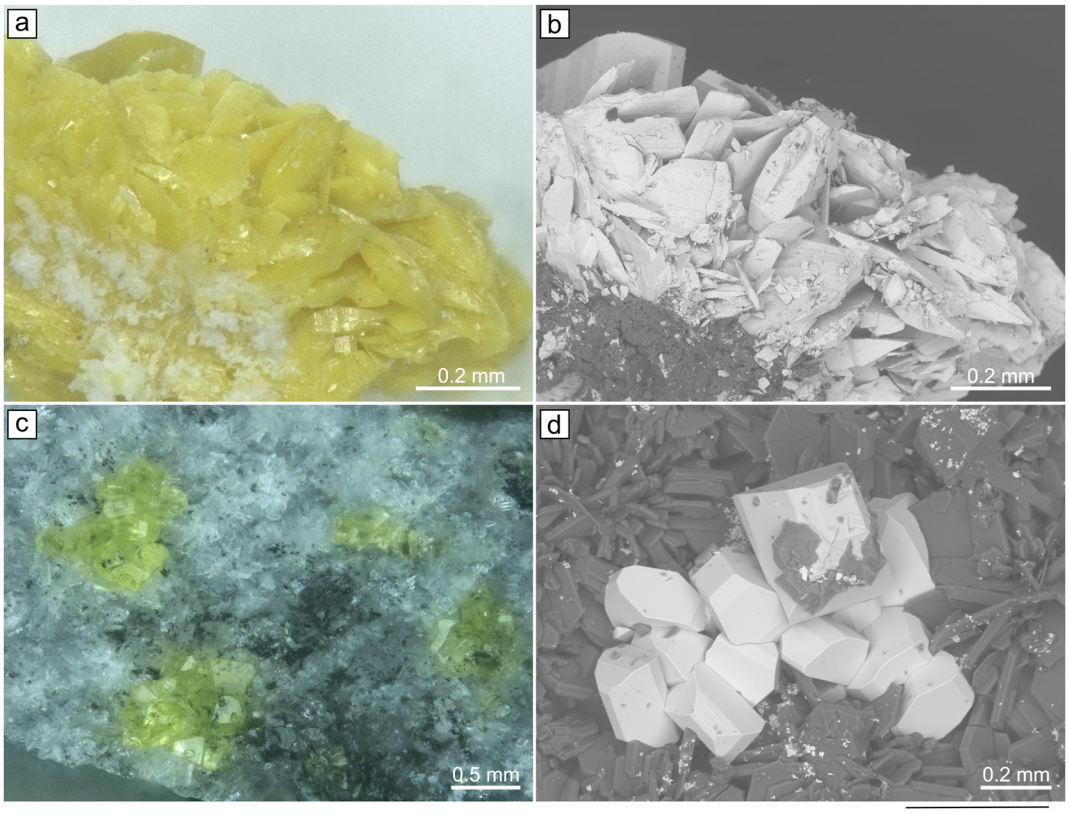

Figure 1: The images of yellow platy crystals of soddiyte (a,b) and yellow prismatic crystals of $Na_2(UO_2)_2(SiO_4)F_2$ (c,d) under optical microscope and BSE.

Table 1: Crystallographic data and refinement parameters for soddiyte and $Na_2[(UO_2)_2(SiO_4)F_2]$.

	soddyite	**$Na_2[(UO_2)_2(SiO_4)F_2]$**
Temperature (°C)	25	
Radiation	MoKα, 0.71073 Å	
Crystal system	Orthorhombic	Tetragonal
Space group	*Fddd*	$I4_1/amd$
a (Å)	8.3246(4)	6.9749(2)
b (Å)	11.2245(5)	
c (Å)	18.6734(6)	18.2807(12)
Volume (Å^3)	1744.83(13)	889.34(8)
d_{calc} (g/cm^3)	5.057	5.348
μ (mm^{-1})	37.246	36.658
Crystal size (mm)	0.05 × 0.06 × 0.14	0.03 × 0.5 × 0.11
θ Range (°)	4.24–27.37	4.44–27.89
h, *k*, *l* ranges	−9 → 10, −14 → 11, −24 → 23	−8 → 8, −6 → 9, −24 → 12
Total reflections collected	2042	1256
Unique reflections (R_{int})	0.024	0.020
$R_1[F > 4\sigma F]$, $wR_1[F > 4\sigma F]$	0.022, 0.054	0.014, 0.030
R_{all}, wR_{all}	0.026, 0.055	0.018, 0.031
Goodness-of-fit	1.133	1.088

AZtecLive STD system of analysis. Analytical conditions were: accelerating voltage 20 kV and beam current 5 nA. Only U, Si and O were recorded, contents of other elements with atomic numbers higher than that of beryllium were below detection limits. The following standards and X-ray lines were used: Si–SiO_2, K_α; U–UO_2, M_β.

The chemical composition of soddyite is (wt%, H_2O content calculated by stoichiometry): SiO_2 8.87, UO_3 85.93, H_2O 5.39, total 100.19. The empirical formula based on 8 O *apfu* and 2 H_2O molecules is $U_{2.01}Si_{0.99}O_8(H_2O)_2$.

Qualitative electron microprobe analysis of ***NAUSIF*** carried out using TM3000 (Hitachi, Tokyo, Japan) revealed no other elements, except U, Si, F and Na, with an atomic number greater than 11 (Na).

2.5 Powder X-ray analysis

The PXRD of $Na_2[(UO_2)_2(SiO_4)F_2]$ and soddyite were studied in air by means of a Rigaku Ultima X-ray diffractometer (Cu-Kα radiation). The samples were prepared using heptane.

The speed of the experiment is 2°/min. Unit-cell parameters were refined by least-square methods.

2.6 High-temperature X-ray powder diffraction study

Thermal behavior of soddyite was studied in air by means of a Rigaku Ultima X-ray diffractometer (Cu-Kα radiation) with a high-temperature camera Rigaku HTA 1600. The samples were prepared from heptane's suspension on a Pt–Rh plate. The temperature step was 20 °C in the range of 25–1,000 °C. Unit-cell parameters at different temperatures were refined by least-square methods. Main coefficients of the thermal expansion tensor were determined using linear approximation of temperature dependences by the ThetaToTensor program.[27]

2.7 Infrared spectroscopy

In order to obtain infrared (IR) absorption spectra (Figure S1), powdered samples of ***NAUSIF*** and soddyite have been mixed with dried KBr, pelletized, and analyzed using an ALPHA FTIR spectrometer (Bruker Optics) with a resolution of 4 cm^{-1}. 10 Scans were obtained. The IR spectrum of an analogous pellet of pure KBr was used as a reference.

3 Results

3.1 Crystal structure of $Na_2(UO_2)_2SiO_4F_2$ and soddyite

In the both soddyite and ***NAUSIF*** structures, a single symmetry unique uranium atom contributes to a typical uranyl cation (*Ur*; <U-O_{ap}> = 1.773 Å). In soddyite (Figure 2a), it is coordinated, in the equatorial plane, by four oxygen atoms from the silicate tetrahedra (<U-O_{eq}> = 2.250 Å) and water molecule (U–H_2O = 2.415 Å) with formation of a *Ur*$O_4(H_2O)$ pentagonal bipyramid. In ***NAUSIF***, water molecule is replaced by a fluoride anion (<U-O_{eq}> = 2.373 Å, U–F = 2.211 Å) and an *Ur*O_4F polyhedron is formed (Figure 2b). The silicon atoms center the typical SiO_4 tetrahedra (<Si–O> = 1.634 and 1.611 Å for soddyite and ***NAUSIF***, respectively). In the latter structure, the sodium cations reside in the *trans*-NaO_4F_2 octahedra (<Na–O> = 2.290 Å, <Na–F> = 2.777 Å) (Figure 2c).

The bond-valence sums, calculated using the parameters from Gagne and Hawthorne[28] correlate well to the formal valences of the atoms (Table S1). The slight overbonding for the silicon atoms is rather commonly observed among the structures of uranyl silicates.[29,30]

In both structures, the UO_7 polyhedra share edges to form chains (Figure 2d and e) rather common for uranium minerals.[8] The silicate tetrahedra decorate these chains sharing edges with the UO_7 bipyramids so that the latter feature a single terminal vertex occupied by water molecule in the structure of soddyite (Figure 2d), and by F- in ***NAUSIF*** (Figure 2e). As a result, either neutral $[(UO_2)_2(SiO_4)(H_2O)_2]$ or negatively charged $[(UO_2)_2(SiO_4)F_2]^{2-}$ chains are formed. These chains link via the opposite edges of the silicate tetrahedra to form microporous frameworks with channels of 3.84 × 4.51 Å and 3.80 × 4.55 Å, respectively (Figure 3). In ***NAUSIF***, the channels are occupied by sodium cations.

Soddyite is orthorhombic (*Fddd*), while ***NAUSIF*** is tetragonal ($I4_1/amd$). In the former structure the chain propagation directions intersect at the acute angle of 73° (Figure 3b), while in the latter, this angle is 90° (Figure 3d). Note that the soddyite structure, after weeksite,[31] is just a second example of a microporous framework among uranyl silicate minerals.

3.2 Single crystal X-ray HT study of NAUSIF

A polythermal single-crystal X-ray experiment for ***NAUSIF*** was conducted in the 25–725 °C range with an increment of 50 °C, and the structure was refined at each step (see the cif files in Supplement). The compound is stable until its melting point of 625 ± 25 °C. Thermal dependences of its unit-cell parameters can be satisfactorily described by linear functions, $a(T) = 6.957 + 0.052 \times 10^{-3}T$, $c(T) = 18.283 + 0.009 \times 10^{-3}\,T$, $V(T) = 885.1 + 13.8 \times 10^{-3}\,T$ (Figure 4)

The thermal expansion of ***NAUSIF*** is strongly anisotropic ($\alpha_{11} = 7.0$, $\alpha_{33} = 1.0$, $\alpha_V = 15 \times 10^{-6}\ K^{-1}$). It is underpinned by the anisotropy of thermal evolution of bond lengths and angles in the coordination polyhedra. In UO_7, upon heating from 25 to 625 °C, the elongation of uranyl bonds is within the standard deviation of 0.003 Å; the U1–O1 bonds, aligned along *a*, expand twice as less (Δd = 0.014 Å) compared to U1–O1, aligned nearly along *c* (Δd = 0.027 Å). In the meantime, the U–F1 bond lengths remain nearly invariable (Δd = 0.005 Å). The same is true for the strong covalent Si–O bonds (Δd = 0.002 Å). The thermal expansion of the NaO_4F_2 octahedra is strongly anisotropic. Their main axes form a 50° angle towards *c*. The elongation rate for the Na–F bonds (Δd = 0.069 Å) is nearly thrice above that of Na–O2 (Δd = 0.025 Å). Between 25 and 625 °C, the O2–O2 edge lengths increase from 3.380 to 3.442 Å. The edge lengths in the UO_6F polyhedra also increase anisotropically. The O1–O1 edge,

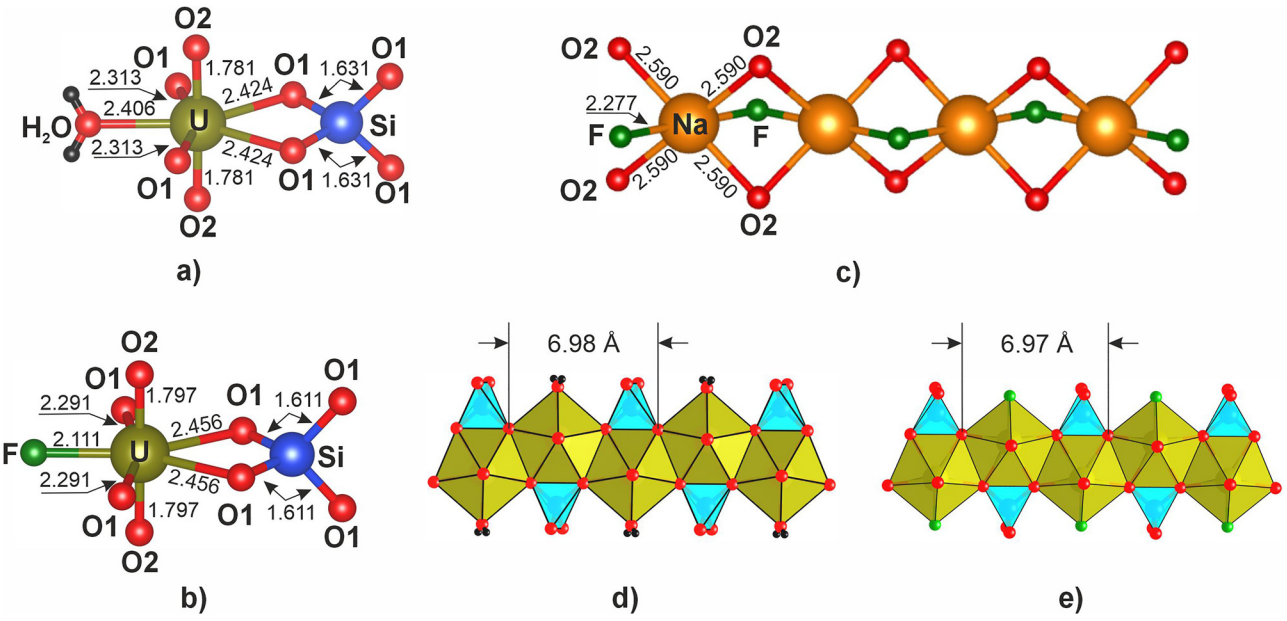

Figure 2: Coordination environments of atoms in soddyite and ***NAUSIF***. U^{6+} and Si^{4+} coordination in the structure of soddyite (a) and ***NAUSIF*** (b) coordination of Na^{+} in chains in ***NAUSIF*** (c) uranyl silicate chains in soddyite (d) and ***NAUSIF*** (e).

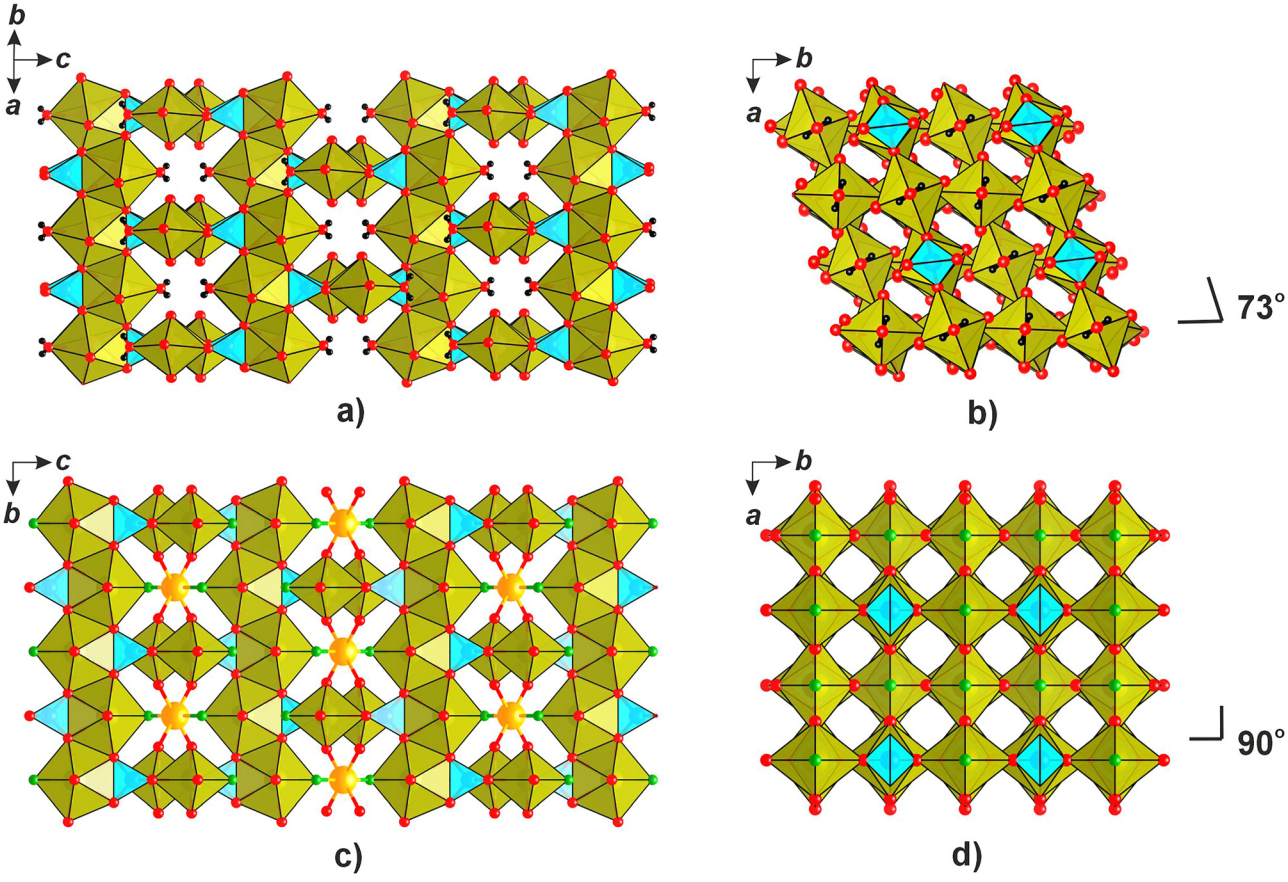

Figure 3: Projections of the soddyite structure along [112] (a) and onto *ab* plane (b); projections of ***NAUSIF*** structure onto *bc* (c) and *ab* (d) planes. Angles between the directions of chain propagation are also indicated.

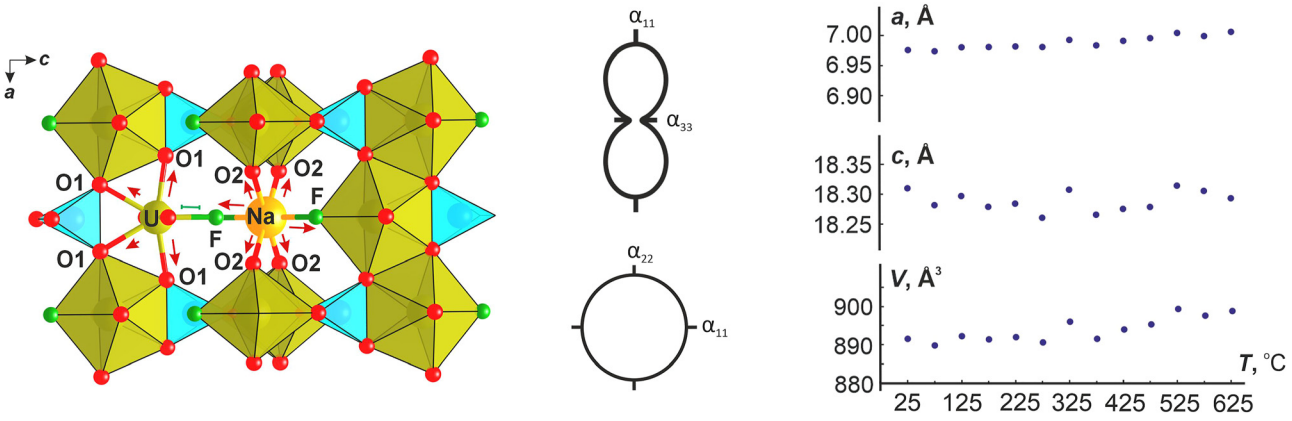

Figure 4: Projection of the ***NAUSIF*** onto *ac*, thermal dependences of the unit-cell parameters and sections of thermal expansion tensors. Arrows indicate the changes in bond lengths in the polyhedra upon heating (red = expansion; green = nearly constant). The error bars are smaller than the size of markers.

shared by the UO_6F and SiO_4 polyhedra, increases from 2.45 to 2.54 Å. The O1-U1-O1 changes from 162.89 to 163.85°.

3.3 Thermal expansion of soddyite studied by powder X-ray diffraction

The mineral is stable until 325 ± 25 °C. Between 325 and 640 °C, the PXRD pattern contain just several weak reflections; above 640 °C, crystallization of U_3O_8 is observed (Figure 5a). Upon heating, the positions of soddyite reflections shift essentially which is caused mainly by the dehydration.

Thermal dependences of unit cell parameters are satisfactorily described by second-order polynomials (Figure 5b). Upon heating, the *b* and *c* decrease while *a* increases. The thermal expansion is also strongly anisotropic; the structure shrinks along *b* and expands along *a*. In fact, the orthorhombic (*Fddd*) *a* call parameters *b* tend to approach the same value of *ca.* 9 Å, which is the tetragonal cell parameter for ***NAUSIF***. Yet, the symmetry remains orthorhombic in the whole temperature interval (Figure 6). Increase of the symmetry upon heating is a commonly observed phenomenon,[32] frequently due to hinge of shear deformations of the structure.

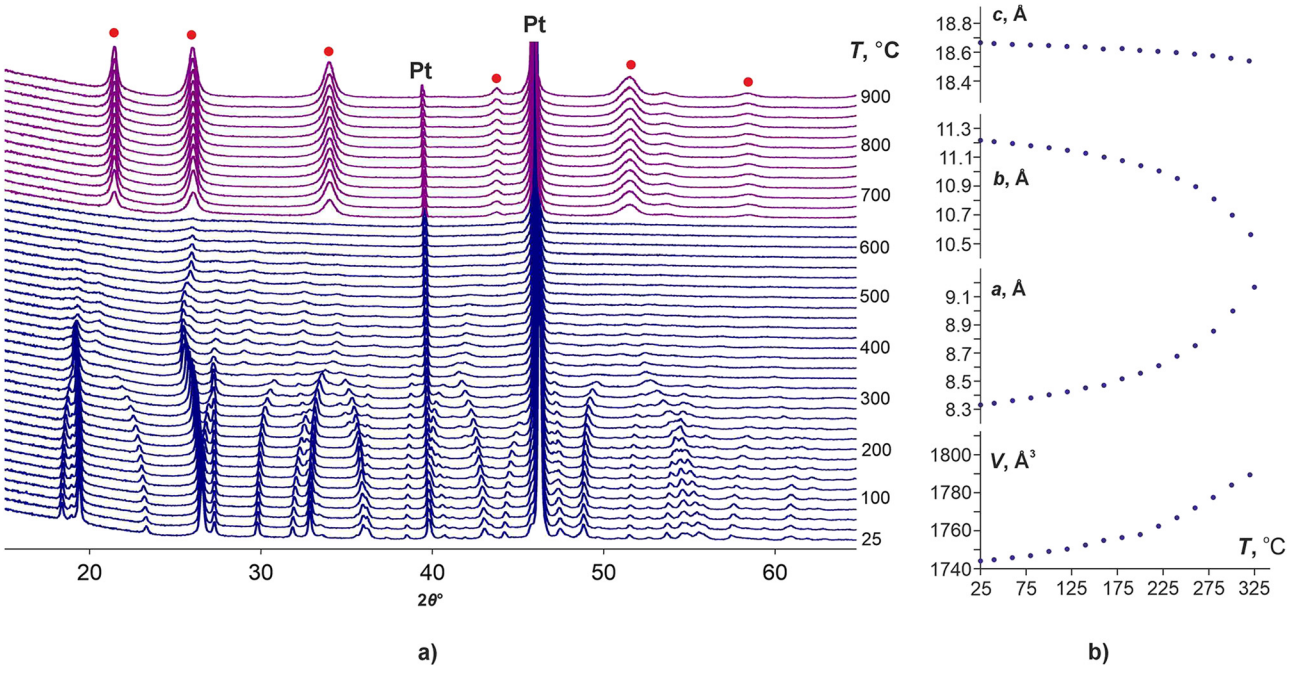

Figure 5: Thermal evolution of PXRD pattern of soddyite (a) and thermal dependence of its unit-cell parameters (b). The U_3O_8 reflections are highlighted in red. The error bars are smaller than the size of markers.

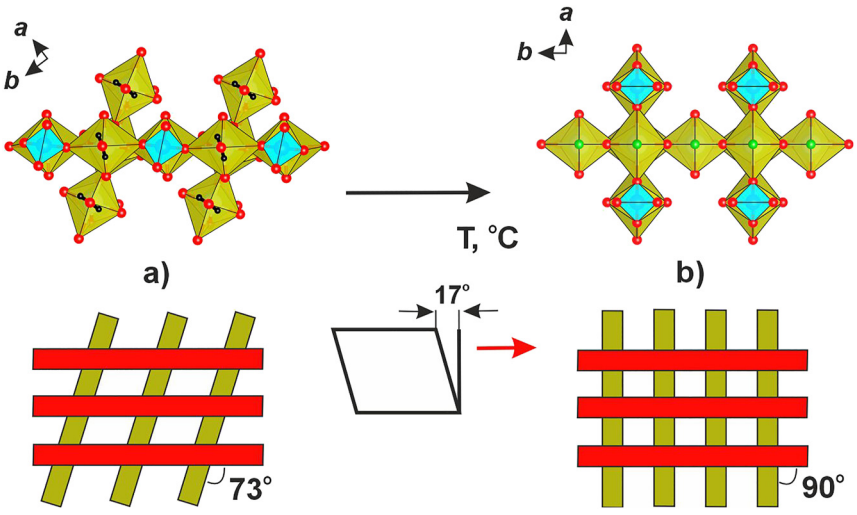

Figure 6: Chain linkage in the structures of soddyite (a) and ***NAUSIF*** (b). The hinge deformation is represented schematically below.

As noted above, the frameworks in the structures of soddyite and ***NAUSIF*** exhibit the same topology yet the angles between chain propagation directions are different. It is reasonable to suggest that upon increasing temperature, the orthorhombic framework of soddyite tends towards tetragonal symmetry with this angle increasing from 72 to 90°. Note that at elevated temperatures, the *a* and *b* unit-cell parameters of soddyite are related to the tetragonal *a* parameter of ***NAUSIF*** approximately by factors of $\sqrt{2}/2$ and $\sqrt{2}$, respectively.

4 Concluding remarks

In the current work, we investigated, for the first time, the thermal behavior of soddyite (via powder XDR) and a related compound ***NAUSIF*** (via single-crystal X-ray diffraction). The former is stable until 325 ± 25 °C, while the latter, until 625 ± 25 °C. Based on the structural data, we suggest a way of approximating anisotropy of thermal expansion. Despite the topological similarity of the frameworks, the thermal stability and expansion parameters of soddyite and ***NAUSIF*** are essentially different. For the latter, thermal expansion is not so anisotropic as for the former. Thermal evolution of the mineral suggests the presence of hinge or shear deformations so that the structure approaches a higher symmetry; that of ***NAUSIF*** exhibits a moderate anisotropy of thermal expansion. These differences can be explained considering change of chemical composition of the mineral due to water release and presence of sodium cations in the channels in ***NAUSIF***. Reference data on soddyite revealed two steps of mass loss upon heating, water release at 300–460 °C, and oxygen evolution at 640–740 °C. In general, our data agree to these observations except that some weak reflections persist in the 325–640 °C range which may indicate stepwise transformation. Formation of U_3O_8 above 640 °C agrees to the previous reports.

Studies on oxidation of uraninite, as well as of SNF[4,33] indicate that UO_2 is unstable under acidic conditions and the rate of its transformation can be quite high. The most common oxidation products are schoepite $(UO_2)_8O_2(OH)_{12}(H_2O)_{12}$, uranophane $Ca[(UO_2)(SiO_3OH)]_2(H_2O)_5$, boltwoodite $(K,Na)[(UO_2)(SiO_3OH)](H_2O)_{1.5}$, soddyite $(UO_2)_2(SiO_4)(H_2O)_2$, and compreignacite $K_2(UO2)_6O_4(OH)_6(H_2O)_7$. Abundant formation of soddyite upon oxidation of uraninite was observed in Nevada (Yucca Mountain) with intermediate formation of becquerelite.[2,3]

Certain nuclides like ^{237}Np,[34,35] ^{135}Cs, ^{137}Cs,[36] and ^{90}Sr[37] can accumulate in uranyl compounds. For their immobilization, minerals with microporous structures are considered to be more preferable.[34–37] Among uranyl silicates, these are weeksite and soddyite. Klingensmith et al. [35] reported incorporation of NpO_2^+ into synthetic soddyite with concomitant introduction of Na^+ into the channels, to keep the charge balance: $(UO_2)_{2-x}(NpO_2)_xNa_xSiO_4{\cdot}2H_2O$.

According to Weck et al. [38] soddyite is unstable under oxidizing conditions and transforms into studtite. One can suggest that the electroneutral framework containing only relatively weakly bound water molecules is prone to transformations, possible via an exchange route. Our polythermic studies demonstrate that soddyite decomposes above 325 °C. Some analogies can be traced to the thermal behavior of certain zeolites.[39] On the other hand, **NAUSIF** is stable until 625 °C. Substitution of readily exchangeable (and expellable upon heating) neutral water molecules in the uranium coordination sphere by more strongly bound fluorine atoms and further linkage of the structure by the sodium cations in the channels essentially stabilizes the structure motif. Note that the synthesis conditions for the artificial soddyite and

NAUSIF are similar, and both compounds can crystallize during one experiment (Wochten et al., 1997). Considering simultaneous presence of soddyite and boltwoodite, $(K,Na)[(UO_2)(SiO_3OH)](H_2O)_{1.5}$, one could suggest formation of **NAUSIF** during oxidation of uranium deposits in the presence of F^-. Comparison of soddyite and **NAUSIF** suggests that the latter compound is more promising for the immobilization of radionuclides.

Acknowledgments: Technical support by the X-Ray Diffraction and Geomodel Resource Centers of Saint-Petersburg State University is gratefully acknowledged.
Research ethics: Not applicable.
Informed consent: Not applicable.
Author contributions: The authors have accepted responsibility for the entire content of this manuscript and approved its submission.
Use of Large Language Models, AI and Machine Learning Tools: None declared.
Conflict of interest: The authors state no conflict of interest.
Research funding: This work was financially supported by the Russian Science Foundation through the grant 23-27-00153.
Data availability: The raw data can be obtained on request from the corresponding author.

References

1. Plášil, J. Oxidation-hydration Weathering of Uraninite: the Current State-Of-Knowledge. *J. Geosci.* **2014**, *59*, 99–114.
2. Wronkiewicz, D. J.; Bates, J. K.; Gerding, T. J.; Veleckis, E.; Tani, B. S. Uranium Release and Secondary Phase Formation during Unsaturated Testing of UO_2 at 90 °C. *J. Nucl. Mater.* **1992**, *190*, 107–127.
3. Wronkiewicz, D. J.; Bates, J. K.; Wolf, S. F.; Buck, E. C. Ten-year Results from Unsaturated Drip Tests with UO_2 at 90 °C: Implications for the Corrosion of Spent Nuclear Fuel. *J. Nucl. Mater.* **1996**, *238*, 78–95.
4. Finch, R. J.; Buck, E. C.; Finn, P. A.; Bates, J. K. Oxidative Corrosion of Spent UO_2 Fuel in Vapor and Dripping Groundwater at 90 °C. *Mater. Res. Sympos. Proc.* **1999**, *556*, 431–438.
5. Trocellier, P.; Cachoir, C.; Guilbert, S. Dissolution of Uranium Dioxide in Granitic Groundwater by Secondary Phase Formation. *J. Nucl. Mater.* **1998**, *256*, 197–206.
6. Gob, S.; Guhring, J. E.; Bau, M.; Markl, G. Remobilization of U and REE and the Formation of Secondary Minerals in Oxidized U Deposits. *Am. Mineral.* **2013**, *98*, 530–548.
7. Belova, L. N.; Doynikova, O. A. Conditions of Formation of Uranium Minerals in the Oxidation Zone of Uranium Deposits. *Geol. Ore Depos.* **2003**, *45*, 148–152.
8. Krivovichev, S. V.; Plášil, J. Mineralogy and Crystallography of Uranium. In *Uranium: From Cradle to Grave*; Burns, P. C., Sigmon, G. E., Eds.; Mineralogical Association of Canada Short Courses: Quebec, QC, Canada, Vol. 43, 2013; pp 15–119.
9. Gorman, D. H. Studies of Radioactive Compounds: V – Soddyite. *Am. Mineral.* **1952**, *37*, 386–393.
10. Legros, J. P.; Jeannin, Y. Coordination de l'uranium par l'Ion germanate. II. Structure du germanate d'uranyle dihydraté $(UO_2)_2GeO_4(H_2O)_2$. *Acta Crystallogr.* **1975**, *31*, 1140–1143.
11. Kuznetsov, L. M.; Tsvigunov, A. N.; Makarov, E. S. Hydrothermal Synthesis and Physico-Chemical Study of the Synthetic Analog of Soddyite. *Geochimiya* **1981**, *10*, 1493.
12. Moll, H.; Matz, W.; Schuster, G.; Brendler, E.; Bernhard, G.; Nitsche, H. Synthesis and Characterization of Uranyl Orthosilicate $(UO_2)_2SiO_4 \cdot 2H_2O$. *J. Nucl. Mater.* **1995**, *227*, 40–49.
13. Belokoneva, E. L.; Mokeeva, V. I.; Kuznetsov, L. M.; Simonov, M. A.; Makarov, E. S.; Belov, N. V. Crystal Structure of Synthetic Soddyite, $(UO_2)_2[SiO_4](H_2O)_2$. *Dokl. Akad. Nauk SSSR* **1979**, *246*, 93–96.
14. Nozik Y. Z.; Kuznetsov L. M. Neutron Diffraction Study of Synthetic Soddyite by the Full-Profile Analysis Technique, *Kristallografiya* **1990**, *35*, 1563–1564.
15. Demartin, F.; Gramaccioli, C. M.; Pilati, T. The Importance of Accurate Crystal Structure Determination of Uranium Minerals. II. Soddyite $(UO_2)_2(SiO_4) \cdot 2H_2O$. *Acta Crystallogr.* **1992**, *48*, 1–4.
16. Plášil, J. Mineralogy, Crystallography and Structural Complexity of Natural Uranyl Silicates. *Minerals* **2018**, *8*, 551.
17. Čejka, J Infrared Spectroscopy and Thermal Analysis of the Uranyl Minerals. *Rev. Mineral. Geochem.* **1999**, *38*, 521–622.
18. Frost, R. L.; Čejka, J.; Weier, M. L.; Martens, W.; Kloprogge, J. T. A Raman and Infrared Spectroscopic Study of the Uranyl Silicates - Weeksite, Soddyite and Haiweeite. *Spectrochim. Acta* **2006**, *A64*, 308–315.
19. Colmenero, F.; Bonales, L. J.; Cobos, J.; Timóna, V. Structural, Mechanical and Vibrational Study of Uranyl Silicate Mineral Soddyite by DFT Calculations. *J. Solid State Chem.* **2017**, *253*, 249–257.
20. Chernorukov, N. G.; Knyazev, A. V.; Sergacheva, I. V.; Ershova, A. V. Synthesis and Physicochemical Study of Compounds in UO_3-A_kO_k/2 (A_k = B, Si, Ge)-H_2O Systems. *Radiochemistry* **2004**, *46*, 218–223.
21. Serezhkin, V. N.; Rasshchepkina, N. A.; Serezhkina, L. B. Thermal Decomposition of Zinc Uranyl Sulfate and Zinc Selenito Uranylate Hydrates. *Radiokhimiya* **1980**, *22*, 49–52.
22. Sureda, R.; Casas, I.; Gimenez, J.; de Pablo, J.; Quinones, J.; Zhang, J.; Ewing, R. C. Effects of Ionizing Radiation and Temperature on Uranyl Silicates: Soddyite $(UO_2)_2(SiO_4)(H_2O)_2$ and Uranophane $Ca(UO_2)_2(SiO_3OH)_2$ 3-5H_2O. *Environ. Sci. Technol.* **2011**, *45*, 2510–2515.
23. Blaton, N.; Vochten, R.; Peeters, O. M.; van Springel, K. The Crystal Structure of $Na_2(UO_2)_2SiO_4F_2$, a Compound Structurally Related to Soddyite, and Formed during Uranyl Silicate Synthesis in Teflon-Lined Bombs. *Neues Jahrbuch Mineral., Monatsh.* **1999**, *6*, 253–264.
24. Nazarchuk, E. V.; Siidra, O. I.; Charkin, D. O.; Tagirova, Y. G. Framework Uranyl Silicates: Crystal Chemistry and a New Route for the Synthesis. *Materials* **2023a**, *16*, 4153.
25. Sheldrick, G. M. Crystal Structure Refinement with SHELXL. *Acta Crystallogr.* 2015, *C71*, 3–8.
26. Downs, R. T. Analysis of Harmonic Displacement Factors. In *High-Temperature and High-Pressure Crystal Chemistry*; Hazen, R. M., Downs, R. T., Eds.; Mineralogical Society of America, Geochemical Society: Washington, DC, Vol. 41, 2000; pp. 61–87.
27. Bubnova, R. S.; Firsova, V. A.; Filatov, S. K. Software for Determining the Thermal Expansion Tensor and the Graphic Representation of its Characteristic Surface (Theta to Tensor-TTT). *Glass Phys. Chem.* **2013**, *39*, 347–350.
28. Gagné, O. C.; Hawthorne, F. C. Bond-length Distributions for Ions Bonded to Oxygen: Results for the Transition Metals and Quantification of the Factors Underlying Bond-Length Variation in In-Organic Solids. *Acta Crystallogr.* **2016**, *B72*, 602–625.

29. Nazarchuk, E. V.; Siidra, O. I.; Charkin, D. O.; Tagirova, Y. G. Uranyl Silicate Nanotubules in $Rb_2[(UO_2)_2O(Si_3O_8)]$: Synthesis and Crystal Structure. *Z. Kristallogr.* **2023b**, *238*, 349–354.
30. Nazarchuk, E. V.; Siidra, O. I.; Charkin, D. O.; Tagirova, Y. G. U. (VI) Coordination Modes in Complex Uranium Silicates: $Cs[(UO_6)_2(UO_2)_9(Si_2O_7)F]$ and $Rb_2[(PtO_4)(UO_2)_5(Si_2O_7)]$. *Chemistry* **2022**, *4*, 1515–1523.
31. Fejfarová, K.; Plášil, J.; Yang, H.; Čejka, J.; Dušek, M.; Downs, R. T.; Barkley, M. C.; Škoda, R. Revision of the Crystal Structure and Chemical Formula of Weeksite, $K_2(UO_2)_2(Si_5O_{13})\cdot 4H_2O$. *Am. Mineral.* **2012**, *97*, 750–754.
32. Filatov, S. High-temperature Crystal Chemistry. In *Theory*, *Methods and Research Results*; Nedra: Leningrad, 1990; p. 288. (in Russian).
33. Wilson, C. N. *Results From Nevada Nuclear Waste Storage Investigations (NNWSI) Series 3 Spent Fuel Dissolution Tests*; Pacific Northwest Laboratory Report PNL-7170: Richland, Washington, 1990.
34. Burns, P. C.; Klingensmith, A. L. Uranium Mineralogy and Neptunium Mobility. *Elements* **2006**, *2*, 351–356.
35. Klingensmith, A. L.; Burns, P. C. Neptunium Substitution in Synthetic Uranophane and Soddyite. *Am. Mineral.* **2007**, *92*, 1946–1951.
36. Burns, P. C. Cs Boltwoodite Obtained by Ion Exchange from Single Crystals: Implications for Radionuclide Release in a Nuclear Repository. *J. Nucl. Mater.* **1999**, *265*, 218–223.
37. Burns, P. C.; Li, Y. The Structures of Becquerelite and Sr-Exchangedbecquerelite. *Am. Mineral.* **2002**, *87*, 550–557.
38. Weck, P. F.; Kim, E.; Buck, E. C. On the Mechanical Stability of Uranyl Peroxide Hydrates: Implications for Nuclear Fuel Degradation. *RSC Adv.* **2015**, *5*, 79090–79097.
39. Bish, D. L.; Carey, C. B. Thermal Behavior of Natural Zeolites. In *Book: Natural Zeolites: Occurrence*, *Properties*, *Applications*; Bish, D. L., Ming, D. W., Eds.; Mineralogical Society of America: Washington, DC, Vol. 45, 2000; pp. 403–452.

Supplementary Material: This article contains supplementary material (https://doi.org/10.1515/zkri-2024-0091).